us an effective means of studying the nature of boundary scattering of conduction electrons.

ACKNOWLEDGMENTS

We are indebted to the staff of the Computing Center at Tsing Hua University for their assistance in numerical work. One of us (Y.H.K.) would like to thank the members of the Institute of Physics at Tsing Hua for the hospitality extended to him during his sabbatical leave.

*Permanent address: Department of Physics, State University of New York, Stony Brook, N. Y. 11790.

[1]For a recent review, see for example, R. G. Chambers, in *The Physics of Metals*, Vol. I, edited by J. M. Ziman (Cambridge U. P., New York, 1969).

[2]K. Fuchs, Proc. Cambridge Phil. Soc. 34, 100 (1938).

[3]E. H. Sondheimer, Advan. Phys. 1, 1 (1952).

[4]E. Koenigsberg, Phys. Rev. 91, 8 (1953).

[5]M. Ya. Azbel, Dokl. Akad. Nauk SSSR 99, 519 (1954); Zh. Eksperim. i Teor. Fiz. 44, 1262 (1963) [Sov. Phys. JETP 17, 851 (1963)].

[6]E. A. Kaner, Zh. Eksperim. i Teor. Fiz. 34, 658 (1958) [Sov. Phys. JETP 7, 454 (1958)].

[7]T. H. K. Barron and D. K. C. McDonald, Physica 24, S102 (1958).

[8]Y. H. Kao, Phys. Rev. 138, A1412 (1965).

[9]N. C. McGill, Physica 40, 91 (1968).

[10]R. G. Chambers, Proc. Roy. Soc. (London) A202, 378 (1950).

[11]G. E. Reuter and E. H. Sondheimer, Proc. Roy. Soc. (London) A195, 336 (1949).

[12]M. C. Steele, Phys. Rev. 97, 1720 (1955).

[13]J. Babiskin, Phys. Rev. 107, 981 (1957).

[14]A. N. Friedman and S. H. Koenig, IBM J. Res. Develop. 4, 158 (1960).

[15]J. L. Olsen, Helv. Phys. Acta 31, 713 (1958).

[16]M. E. de la Cruz, F. de la Cruz, and J. M. Cotignola (private communication); and Phys. Rev. 163, 575 (1967).

[17]K. L. Chopra, Phys. Rev. 155, 660 (1967).

[18]Yu. P. Gaidukov and Ya. Kadletsova, Zh. Eksperim. i Teor. Fiz. Pis'ma v Redaktsiyu 8, 247 (1968) [Sov. Phys. JETP Letters 8, 151 (1968)].

[19]C. Rau (private communication).

[20]J. E. Parrott, Proc. Phys. Soc. (London) 85, 1143 (1965).

[21]C. S. Lee and Y. H. Kao (unpublished).

PHYSICAL REVIEW B VOLUME 5, NUMBER 6 15 MARCH 1972

Anisotropy of the Threshold Energy for the Production of Frenkel Pairs in Tantalum

Peter Jung and Werner Schilling
Institut für Festkörperforschung, Kernforschungsanlage Jülich, 517 Jülich, Germany
(Received 14 September 1971)

Thin tantalum single-crystal foils with the ⟨110⟩ direction normal to the surface have been irradiated with electrons of energies between 1.0 to 3.2 MeV. By varying the orientation of the foil relative to the direction of the beam over a major part of the fundamental triangle, a strong directional effect in the damage rate was observed for transferred energies of more than 36 eV. In previous measurements especially on the fcc metals copper and gold, much less, if any, anisotropy of the defect production was observed. The data have been corrected for beam spreading due to the finite sample thickness. From the dependence of the defect production on electron energy and foil orientation, the angular dependence of the threshold displacement energy could be fitted. Good over-all fits were only possible when the averaged threshold was about 36 eV in a region of 20° around the ⟨111⟩ direction, about 53 eV in a region of 18° around the ⟨100⟩ direction, and larger than 130 eV in other directions. The existence of such "windows" along the close-packed directions indicates a sequence of replacement collisions which eventually leads to a stable defect. Computer calculations by the Brookhaven group for bcc iron yielded similar threshold windows around the principal crystallographic directions. However, the ratio of the threshold values for the ⟨100⟩ and ⟨111⟩ directions obtained by this group does not agree with our result. For the lowest threshold energy in tantalum, we found 32 ± 2 eV, and for the electrical resistivity per unity concentration of Frenkel pairs, we obtained $(17 \pm 3) \times 10^{-4}$ Ω cm.

I. INTRODUCTION

Irradiation of a crystal with fast electrons results in a transfer of recoil energy to the lattice atoms. If this recoil energy exceeds a certain threshold value T_d, the struck atom can be displaced permanently from its lattice site, leaving behind a vacancy. Besides this vacancy, an interstitial is produced at some distance via replacement collisions. The interstitial together with the vacancy is called a Frenkel pair.

The atomic structure of the lattice causes the threshold energy to depend on the direction of the knocked-on atom. Therefore, in single-crystal

samples the defect-production rate should vary with the direction of the incident electron beam. A great deal of experimental work on the directional dependence of radiation damage has been done on silicon single crystals.[1] With this material for the first time a technique was used in which the orientation dependence of the damage rate was investigated by rotating the sample with respect to the incident beam.[2] An interpretation of these measurements in terms of an anisotropic threshold energy is given in Refs. 3–5.

Previous single-crystal experiments with metals have been performed with copper, [6,7] gold,[8] iron,[9,10] and cobalt.[11,12] In contrast to silicon, in all these experiments thin single-crystal foils of different orientation were rigidly mounted in front of the electron beam and irradiated at low temperatures. In this manner the energy dependence of the defect-production rate could be obtained only for selected orientations. The measurements of Sosin and Garr[6] on copper and the measurements of Bauer and Sosin[8] on gold gave only small differences in the defect production for the three principal crystallographic directions. However, these data and especially those of Kamada *et al.*[7] were strongly influenced by the finite thickness of the samples used and by variations of the sample thickness over the irradiated area. Because of similar uncertainties in the sample and irradiation geometries, Lomer and Pepper[9,10] could not give reliable absolute values of the damage rates for their iron single crystals.

For these reasons the conclusions drawn so far from a comparison of the absolute damage rates observed for different samples with different orientations must be viewed with caution.

The straightforward way to determine at least the minimum threshold energy is to extrapolate the damage rates obtained for samples of different orientations as a function of electron energy to zero damage rate. However, such a procedure encounters the difficulty that very thin samples would be required in which size-effect corrections may strongly influence the observed damage rates[13] and that unexplained subthreshold effects[14] which are probably connected with impurities seriously impede an unambiguous extrapolation of the "true intrinsic" damage rate to zero.

In order to obtain reliable information about the orientation dependence of the threshold energy, it is therefore necessary to measure precisely the absolute value of the damage rate as a function of sample orientation at electron energies which are high enough that subthreshold effects and size-effect corrections can be neglected. From a comparison of these data with calculations of the orientation dependence of the damage rate based on different profiles of the threshold-energy surface, rather detailed information about the anisotropy of T_d can be obtained. In our investigation of T_d we have measured the defect-production rate as a function of electron energy for many crystal directions using only a few single-crystal samples which were rotated with respect to the incident beam thus excluding possible uncertainties in irradiation and sample geometries. From these data we were able to deduce unambiguously the threshold energies over the whole fundamental triangle.

II. EXPERIMENTAL DETAILS

The samples were made from 15-μm cold-rolled foils of high-purity tantalum (99.995%, A. D. Mackay Inc., New York). They were first decarburized at 2200 °C in 2×10^{-5} Torr of oxygen and then degassed for some minutes at 2500 °C and 10^{-8} Torr.[15]

Laue pictures showed large single-crystal grains (up to 1 cm^2 in size) with ⟨110⟩ orientation normal to the foil surface and little mosaic structure within the grains. From these regions strips were cut along preselected directions, preferably along the ⟨100⟩ and ⟨110⟩ directions. Two such strips were then mounted parallel to each other on a special holder. Potential leads made of 50-μm tantalum wires were spot welded to the samples.

For the irradiations the sample holder was inserted into a special irradiation cryostat.[16] In this cryostat the samples rested in a flat chamber between two stainless-steel windows of 12-μm thickness. This chamber could be flooded with liquid helium supplied from a helium refrigerator. (Details of the irradiation techniques are given in Ref. 17.) The sample chamber together with the samples could be rotated around a vertical axis by about 50° in each direction.

The irradiations were done at 4.5 °K with a beam intensity of 3×10^{17} electrons/cm^2 sec (homogeneity about 3%). After irradiation-time intervals of 10 min, the orientation of the samples was changed by angular steps of 5° and the electrical-resistivity increase was recorded. The measurements at all angular positions were repeated cyclically.

Before each irradiation of tantalum samples, aluminium wires of 0.2-mm diam and of 99.999% purity were irradiated at the same position. In the manner, using the absolute measurements of the damage rates of aluminium as a function of electron energy by Wurm,[18] the electron-beam intensity at the position of the samples could be calibrated. Due to backscattering and secondary-electron emission in the beam-monitoring systems and due to beam spread in the sample chamber, the signals of a Faraday cup placed behind the sample chamber and of a Faraday cup which could be positioned in front of the sample chamber could be used only as relative measures for the beam intensity. From the

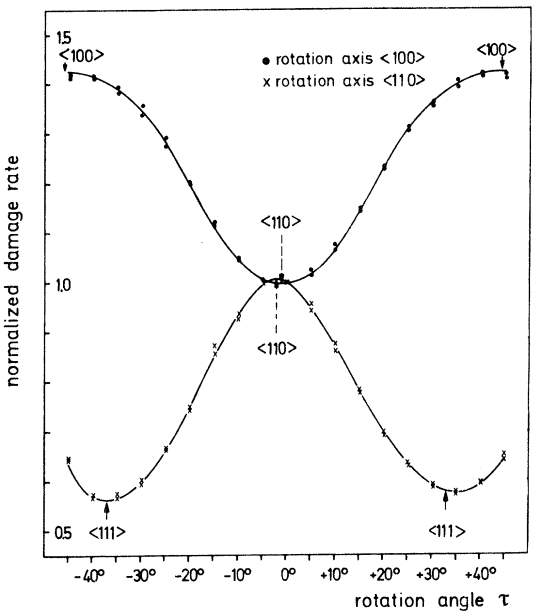

FIG. 1. Normalized damage rates for two tantalum samples with different rotation axes. The arrows indicate positions in which the beam direction was along the indicated crystallographic directions.

damage rates observed for the polycrystalline aluminium wires, it could be confirmed that no measurable change in the electron flux was introduced by the rotation of the whole sample chamber.

III. EXPERIMENTAL RESULTS

In Fig. 1, typical curves for the variation of the damage rate with the rotation angle τ are shown for two samples with rotation axes along the ⟨110⟩ and ⟨100⟩, directions, respectively. Many similar curves have been obtained also for other electron energies and other crystallographic directions of the rotation axis. The damage rates shown in Fig. 1 have been normalized to the damage rate observed for rotation angle zero. This normalization procedure is necessary to eliminate saturation effects in the defect production. These saturation effects give rise to a reduction of the effective defect-production rate with increasing defect density during the course of the irradiation. However, in our experiments we have found that for all orientations of the samples with respect to the incident beam, the relative reduction of the damage rate with increasing defect density, i.e., with increasing radiation-induced resistivity $\Delta\rho$, is the same. Therefore, the ratio of two damage rates for different orientations is independent of saturation effects if both damage rates are taken at equal values of $\Delta\rho$. The data points shown in Fig. 1 all correspond to ratios of experimental damage rates which have been interpolated to identical values of $\Delta\rho$.

For zero rotation angle the direction of the incident electron beam in both samples is almost along ⟨110⟩. The small shifts of the points of symmetry of the observed damage-rate curves with respect to zero rotation angle in Fig. 1 are due to small misalignments of the samples on the holder and can easily be corrected. For the sample with the ⟨110⟩ rotation axis at 3.0-MeV electron energy, a minimum of the damage rate is observed at about 35°, corresponding to an incidence of the electron beam along the ⟨111⟩ direction. For the sample with a ⟨100⟩ rotation axis, a maximum of the damage is observed at about 45°, corresponding to an incidence of the electron beam along a ⟨100⟩ direction.

The energy dependence of the damage rate observed for irradiation along each of the main crystallographic directions is shown in Figs. 2 and 3. In Fig. 2, absolute values of the damage rates (extrapolated to $\Delta\rho = 0$) are plotted vs the maximum transferred energy.

These values could be reproduced from sample to sample within about 7%. The absolute error of these data is mainly given by the uncertainty of the absolute values of the damage rate of the polycrystalline aluminium used for our flux calibration. This error is estimated to be around 10% by Wurm *et al.*[19] This uncertainty can be avoided by plotting relative values of the damage rates normalized to the damage rate for ⟨110⟩ orientation. This has been done in Fig. 3.

While at high energies the damage rate along ⟨100⟩ is much larger and along ⟨111⟩ is much smaller than the damage rate along ⟨110⟩, these relations reverse below about $T_m \approx 55$ eV. At energies $T_m \lesssim 40$ eV the anisotropy of the observed damage rates is more and more suppressed. This suppression is probably due to the increasing relative contribution of subthreshold effects, which below 40 eV exceed the normal damage rate and which are apparently independent of the orientation of the samples. At electron energies near the threshold, other corrections also become very large, e.g., beam spread, increasing path length, and energy loss. Therefore, the low-energy part of the measurements ($T_m \lesssim 45$ eV) was omitted from further evaluations of the data.

The dashed lines in Figs. 2 and 3 give the damage rates after correction for the spread of the electron beam and will be explained in Sec. IV.

IV. ANISOTROPY OF THRESHOLD ENERGY

The connection between the observed energy and orientation dependence of the damage rate and the orientation dependence of the threshold energy for defect production is governed by the differential cross section for energy transfer from the electrons to the lattice atoms. The maximum transferred

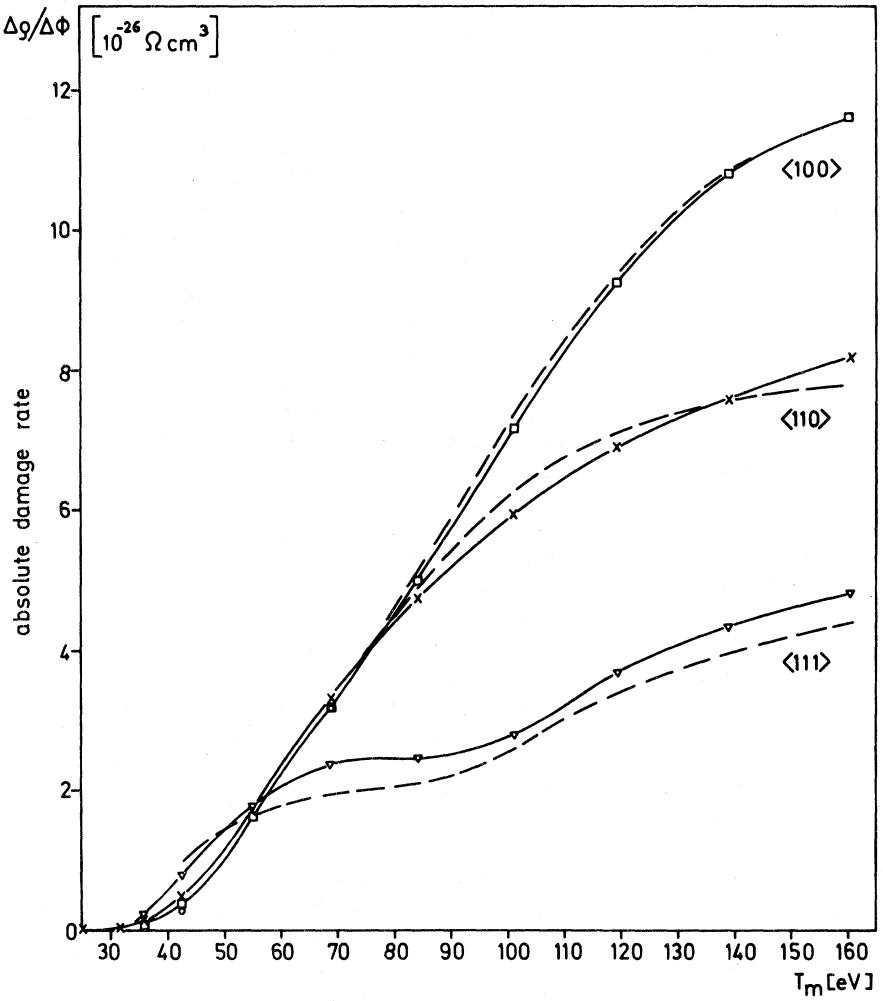

FIG. 2. Absolute damage rate in tantalum as a function of the maximum transferred energy for irradiation along the three main crystallographic directions. The broken lines give the damage rates after correction for the spread of the electron beam.

energy from an electron of energy E to an atom is

$$T_m = 2(m/M)mc^2\,(E'-1)\,, \tag{1}$$

where $E' = [(E/mc^2)+1]^2$ and M and m are the masses of the atom and the electron, respectively. For recoil angle W of the knocked-on atom, the transferred energy is

$$T = T_m \cos^2 W\,, \tag{2}$$

with $0° \leq W < 90°$. The dependence of the scattering probability on W is given by the scattering cross section $d\sigma/d\Omega$, which can be obtained from the McKinley-Feshbach formula with the tabulated corrections from Oen.[20] For the scattering of electrons by the atomic nuclei in the sample, collisions with large recoil angles W and correspondingly small transferred energies T predominate (Coulomb scattering). Therefore, an energetic electron in matter suffers many small deflections which give rise to a spread of the originally parallel beam of electrons. For a survey on this so-called multiple-scattering effect, see Ref. 21. In the following, the theory of Molière[22] is used, which approximates the distribution of the deflection angles α by a Gaussian:

$$G(\alpha) = \frac{2}{\bar{\alpha}\pi^{1/2}}\, e^{-\alpha^2/\bar{\alpha}^2} \tag{3}$$

after the electrons have penetrated a sample of thickness d. The width $\bar{\alpha}$ of the Gaussian shows the following functional dependence[23]:

$$\bar{\alpha}^2 \approx \frac{Z(Z+1)qd}{M}\,\frac{E'}{(E'-1)^2}\,, \tag{4}$$

where q denotes the density of the scattering material. For the 15-μm tantalum foils used, the $\bar{\alpha}$ values are about 25° at 1.5 MeV and 14° at 3.0 MeV.

Another effect of multiple scattering is to increase the path length of the electrons in the sample. According to a theory of Yang,[24] this increase is given by

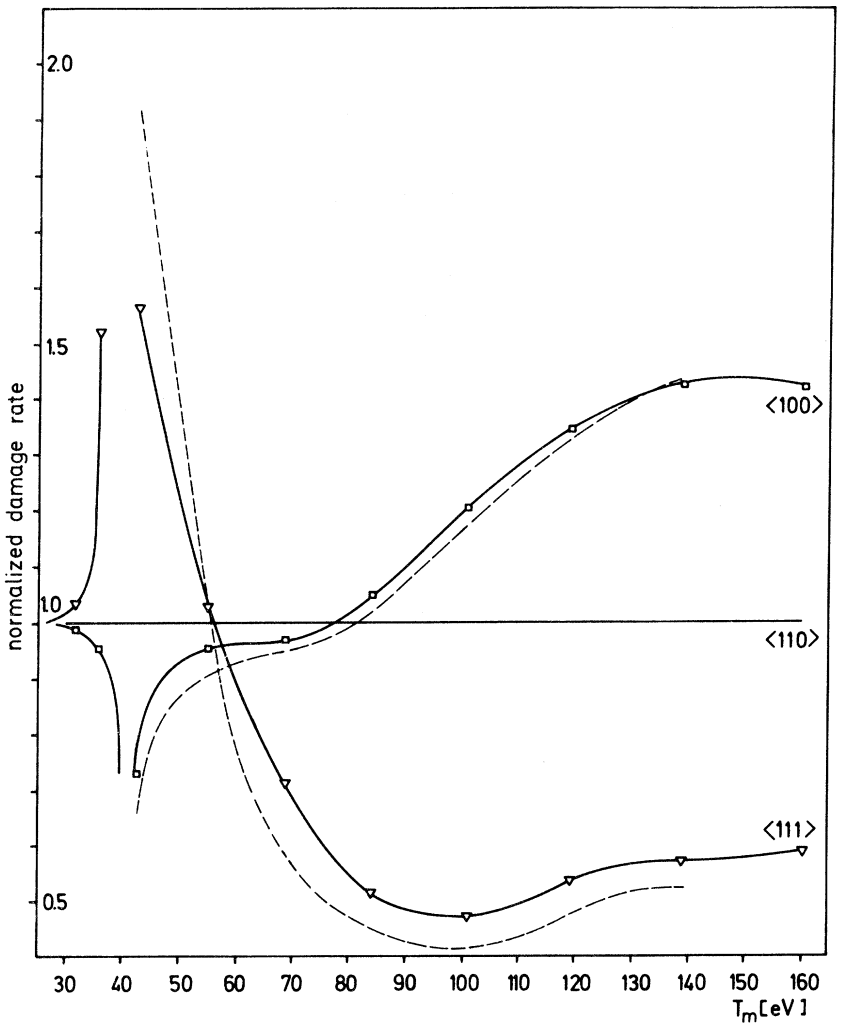

FIG. 3. Ratio of the damage rates in tantalum for irradiation in the main crystallographic directions, normalized to the value for the ⟨110⟩ direction. The broken lines represent the data after correction for beam spread.

$$\Delta d/d = \tfrac{1}{4}\bar{\alpha}^2, \tag{5}$$

The rotation of the samples also causes an increase of the path length. In samples of finite thickness this geometrical effect is not fully compensated by the simultaneous reduction of the number of electrons impinging per cm^2 of the sample. This is due to the increase of $\bar{\alpha}$ with rotation angle τ. For the samples used in our experiments, the corrections calculated according to Eqs. (4) and (5) reduced the observed damage rates by up to 5%.

The next task is to eliminate the effect of beam spread from the experimental data. Since irradiations in many directions of the fundamental triangle have been performed, experimental values of the damage rates were available for all central points of a 5° net work in this triangle or could be obtained by interpolation. With these data it was possible to set up a system of linear equations which connect the measured damage rates $\Delta\rho/\Delta\Phi$ to the ideal damage rates $(\Delta\rho/\Delta\Phi)_{\bar{\alpha}=0}$ for vanishing thickness of the samples:

$$\frac{\Delta\rho}{\Delta\Phi}(\theta_j, \phi_j, E) = \sum_i \left(\frac{\Delta\rho}{\Delta\Phi}(\theta_i, \phi_i, E)\right)_{\bar{\alpha}=0} \times H_{ij}(\bar{\alpha}(E))\cos\theta_i \,\Delta\theta_i \,\Delta\phi_i , \tag{6}$$

with θ_i and ϕ_i characterizing the coordinates of the central point of a network into which the fundamental triangle has been subdivided for the calculation (see Fig. 4). The coefficients $H_{ij}(\bar{\alpha}(E))$ are defined by

$$H_{ij}\, d\Omega_{ij} = G(\alpha_{ij}, \bar{\alpha})\, d\alpha_{ij}, \tag{7}$$

with

$$d\Omega_{ij} = 2\pi \sin\alpha_{ij}\, d\alpha_{ij}, \tag{8}$$

where G is defined by Eq. (3) and α_{ij} measures the angular distance of point i and point j.

For the actual calculation of H_{ij} an average value of G was used taking into account the increase of beam spread $\bar{\alpha}$ through the sample and the fact that for our irradiation geometry, also the spread of the

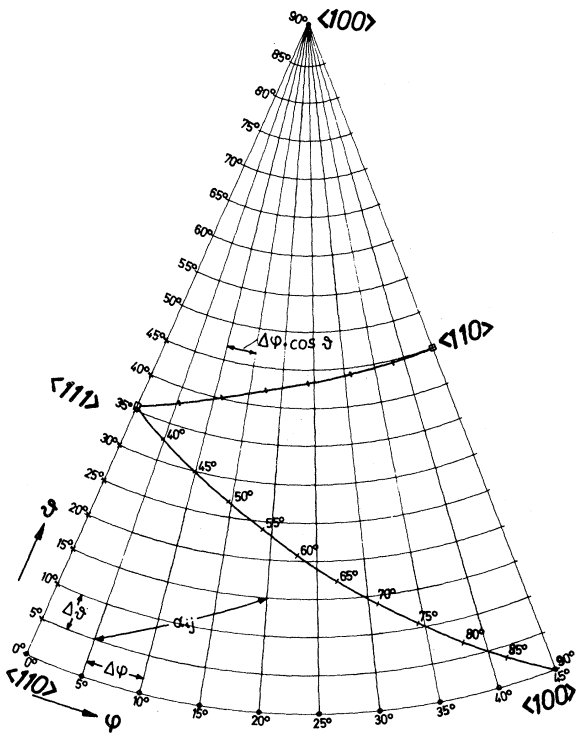

FIG. 4. $5° \times 5°$ network in $\frac{1}{16}$ of space angle with three fundamental triangles of the cubic system.

beam entering the sample is not zero. ($\bar{\alpha}_0$ is about 5° at 3 MeV and 10° at 1.5 MeV.) This is due to scattering of the electron beam in the stainless-steel window and the liquid helium in front of the samples.

The equation system (6) was solved using a digital computer for all electron energies, yielding damage rates for vanishing foil thickness. These values are outlined in Figs. 2 and 3 by the dashed lines which show greater anisotropy than do the uncorrected data points. The corrected damage rates $(\Delta\rho/\Delta\Phi)_{\alpha=0}$ can now be related to the differential cross section $d\sigma$ by

$$\left(\frac{\Delta\rho}{\Delta\Phi}\,(\theta_0, \phi_0, E)\right)_{\bar{\alpha}=0} = \rho_F \int_{T(W,E) > T_d(\theta,\phi)} d\sigma(W, E)\ . \tag{9}$$

Here θ_0, ϕ_0 defines the direction of the incident electron beam and θ, ϕ the direction of the recoil atom with energy T. The displacement energy T_d is assumed to depend on the crystallographic direction θ and ϕ, whereas T and $d\sigma$ depend only on the scattering angle W, i.e., the angular difference between (θ_0, ϕ_0) and (θ, ϕ). The integration over the differential scattering cross section in Eq. (9) is to be taken only over those regions in the solid angle for which the transferred energy T is larger than the displacement energy T_d. This prescription connects the desired orientation dependence of the displacement energy with the observed orientation and energy dependence of the damage rate.

In deducing relation (9), a number of assumptions had to be made: (i) The value ρ_F of the resistivity per Frenkel pair was assumed to be independent of the direction of the displacement process. This can be justified to some extent by the observation that in Al, Cu, Fe, Ni,[25] and Pt[26] the ratio between the stored energy and the resistivity change $\Delta\rho$ is constant through annealing stage I. This suggests that all the different Frenkel-pair configurations annihilating in stage I have nearly equal values ρ_F (and also nearly equal formation energies).

(ii) Multiple displacements are neglected. The experimental study of secondary displacement process in Al by Wurm *et al.*,[19] a critical evaluation of the damage rates observed during heavy-particle irradiation,[27] and the computer simulation of multiple displacements in Fe by Erginsoy *et al.*[28] all suggest that multiple-displacement processes require recoil energies which are higher than about six times the minimum threshold energy for single displacements (i.e., more than about 100 eV in Al and 110 eV in Fe). This observation would suggest that in the range of recoil energies over which Eq. (9) was used for Ta, i.e., from the minimum threshold energy of about 32 eV[15,29] to the maximum recoil energy achieved, 160 eV, the contribution of multiple-displacement processes can be safely neglected.

(iii) The probability for creation of a stable Frenkel pair was assumed to jump from 0 to 1 exactly at a recoil energy $T = T_d(\theta, \phi)$. Model calculations concerning the influence of lattice vibrations[30] and experiments on the influence of impurities and dislocations[7,14] on the displacement process suggest that the probability for displacement in a crystallographic direction (θ, ϕ) is indeed well approximated by a step function.

In order to obtain from the corrected damage rates the orientation dependence of the threshold energy $T_d(\theta, \phi)$, the following procedure was used. With the aid of a digital computer, the theoretical damage rates were calculated from Eq. (9) for different test functions $T_d(\theta, \phi)$. Then the results of this calculation were compared with the experimental damage rates. By variation of $T_d(\theta, \phi)$, a good fit was attempted, first for the principal crystallographic directions and then for other crystallographic directions, at energies of 1.5, 2.0, 2.5, and 3.0 MeV. As a measure of the quality of the fit, the sum of the squared deviations was taken between all experimental and theoretical damage rates weighted by the rms error of the measurements.

For an initial choice of the threshold-energy profile $T_d(\theta, \phi)$, an expansion in cubic harmonics as proposed by van Jan and Seeger[31] for copper was

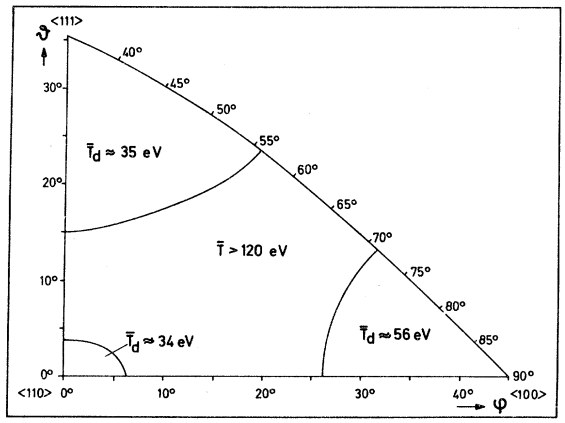

FIG. 5. Simplified threshold-energy profile.

first used. In this case, T_d only depends on three parameters, namely, the thresholds along the principal crystallographic directions. But no sensible fit could be obtained for any choice of these parameters.

As a second starting point for the threshold-energy profile, the results of the computer simulations by Erginsoy *et al.*[32] for bcc iron were used in a simplified manner. These calculations gave rather sharply defined regions around the three principal crystallographic directions with low threshold energies and rather high threshold energies in the region between (see Fig. 6). If the angular extent of these regions is not varied, a fit with such a profile contains four parameters: the three threshold energies in the regions around the main crystallographic directions and a fourth one for the intermediate region. The calculations showed that a reasonable fit was possible only for a profile with a threshold energy in the ⟨100⟩ region exceeding that of the ⟨111⟩ direction and a pronounced maximum of the threshold energy in the remaining part of the fundamental triangle.

In order to improve the fit, we also changed the shape and size of the low threshold regions around the main crystallographic directions. About 20 different profiles were fitted. However, nearly the same magnitude of the four T_d values was always obtained. But the quality of the fit was strongly influenced by changing the size of the regions. A picture of the most satisfactory profile is given in Fig. 5.

Since the assumption of four sharply limited regions with constant threshold-energy values is probably too restrictive, we established a fitting program where the fundamental triangle was subdivided into regions of $5° \times 5°$. The assumption of different T_d values in each region introduces 39 independent parameters which were varied in a least-squares fit.

The result of such a fit is shown on the right-hand side of Fig. 6. A comparison of the damage-rate values calculated for this profile using Eq. (9) with the experimental values corrected for beam spread is shown in Fig. 1. The fit is shown for the absolute and for the normalized damage rates corresponding to the data of Figs. 2 and 3. The threshold-energy surface obtained in this manner exhibits well-defined shallow regions with low threshold energies around the main crystallographic directions,

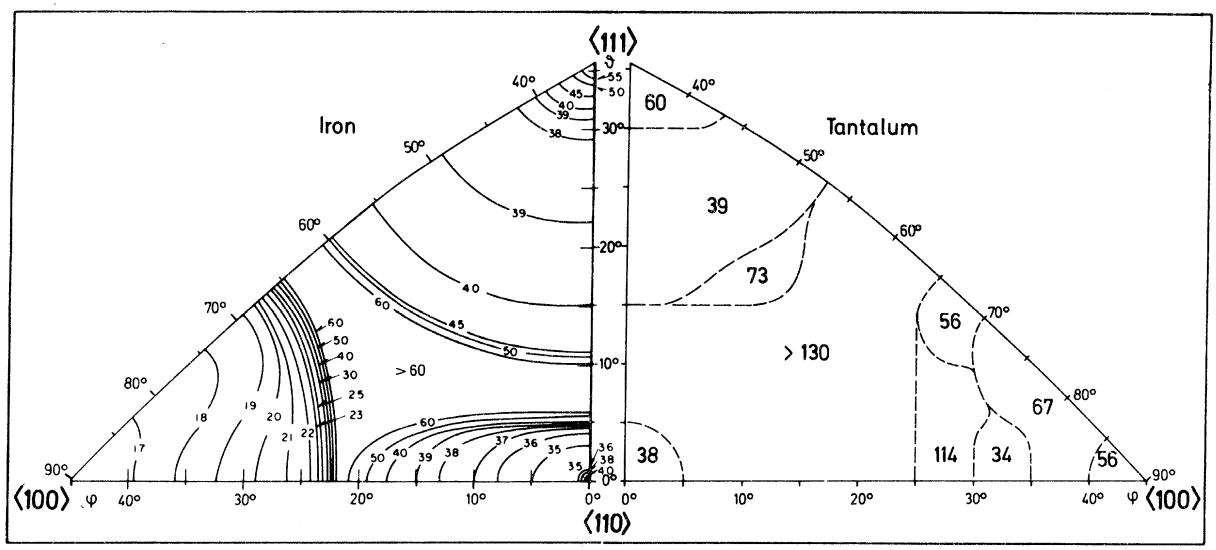

FIG. 6. Threshold-energy profile for bcc iron from computer calculations of Erginsoy *et al.* (Ref. 32) and for tantalum extracted from damage-rate measurements. The figures give the average threshold energies in eV for the particular regions.

while, in the region between, the threshold rises steeply to more than 130 eV. The region around ⟨110⟩ is much smaller and not as well established as those around the other directions, and its contribution to the defect production can be almost neglected at higher electron energies. The low-threshold-energy regions are not circular but are more or less deformed on account of the crystal anisotropy. As in the calculations of Erginsoy *et al.*[32] the displacement energies exactly along the close-packed ⟨111⟩ direction exhibit a small maximum, while the region of minimum threshold energy is ring shaped around this direction. Although in general the results of such a fit must be viewed with great caution because only a local minimum of the set of parameters may be obtained and because the number of open parameters (39) is rather large compared with the number of data points (about 200), we feel that the essential features of the threshold-energy surface given above are rather safely established. This conclusion is based first on the close reproduction of the main topology of the threshold-energy surface deduced from the simplified model shown in Fig. 5 and second on the fact that several runs in which quite different sets of input parameters—all within the error bars of the experimental data—were used gave rather similar threshold-energy profiles.

To give a feeling of this uncertainty in the determination of the threshold energy, in Fig. 8 the contours of such profiles along the border of the fundamental triangle are shown for three different fits, all yielding damage-rate curves lying within the error bars given in Fig. 7. The solid line in Fig. 8 corresponds to the best fit which was shown in Fig. 7 and from which the profile shown in Fig. 6 was deduced. Obviously, all the profiles in Fig. 8 show pronounced minima of the threshold energy around the main crystallographic axis, but the details of the structure in these minimum-energy regions are not always fully reproduced. For the lowest threshold value (32 ± 2) eV was always found in the minimum-energy region near ⟨111⟩. This value agrees well with earlier measurements on polycrystalline tantalum by Messiner[15] and Youngblood *et al.*[29]

If the threshold energy is known in all directions, the total displacement cross section can be calculated according to Eq. (9). Using this calculated total displacement cross section, the increase in the resistivity ρ_F by 1-at.% Frenkel pairs can be obtained from the experimental result. The resulting value of $\rho_F = (17 \pm 3)\ \mu\Omega$ cm lies somewhat above the

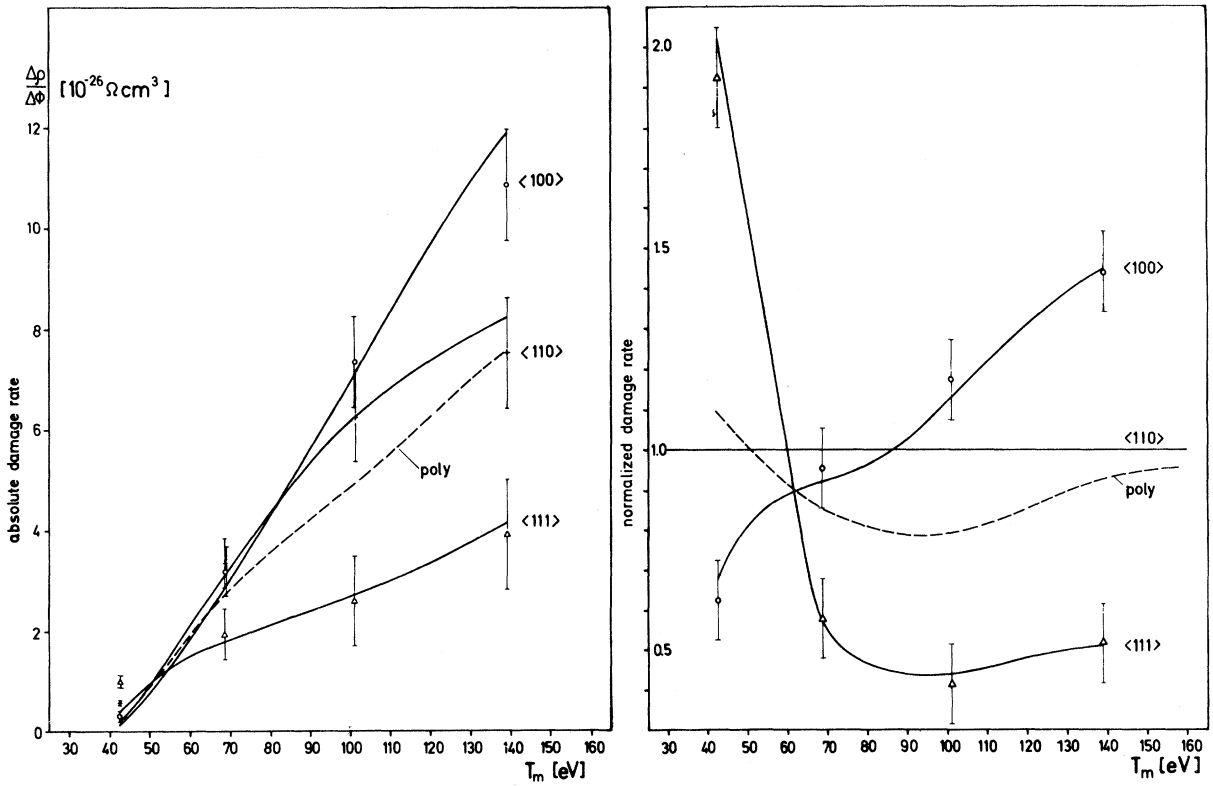

FIG. 7. Comparison of the energy dependence of the damage rates in the main crystallographic directions calculated from the threshold-energy profile of tantalum outlined in Fig. 6 with the experimental values corrected for beam spread. The broken line represents the integrated "polycrystalline" damage rate.

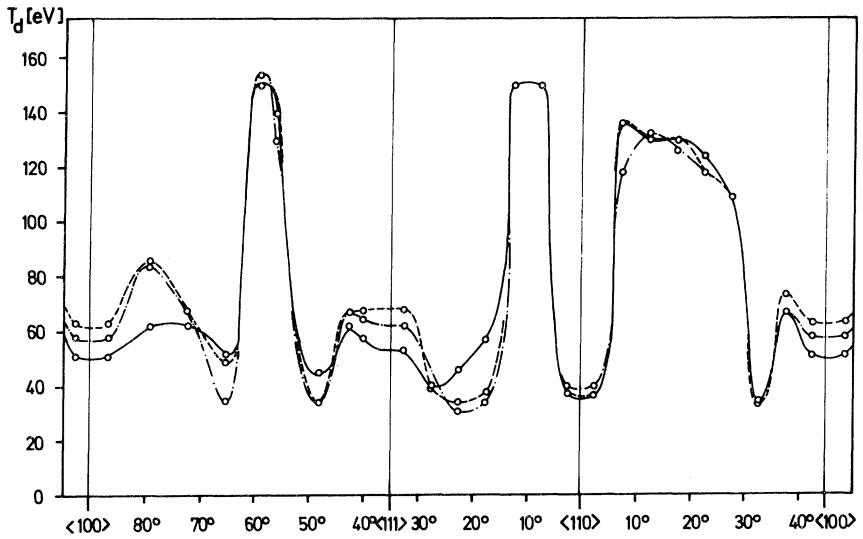

FIG. 8. Contour of the threshold-energy profile along the borders of the fundamental triangle. The curves pertain to three different fits.

value of the thermal resistivity at the Debye temperature (for tantalum: $\rho_{240\,C} = 11.5\ \mu\Omega\,\mathrm{cm}$) which was often assumed to be a good guess for ρ_F.[33]

Channeling of electrons and its influence on multiple scattering[34] and radiation damage[35,36] have been reported. For electrons impinging along close-packed directions Frandson *et al.*[34] observed broadening of the angular distribution of multiple-scattered electrons [see Eq. (3)], and Makin[35] found an increase of the damage observable in Cu in a high-voltage electron microscope at room temperature. The effect of channeling on the distribution of multiple-scattered electrons is appearing, but the difference in the distribution between a close-packed and a random direction is expected to be much less than the variation of the distribution with foil thickness over which we averaged in our calculations. The influence of channeling on radiation damage is not as understandable. First, there are great uncertainties in comparing the electron-microscope investigations (observation of defect loops at room temperature) with our resistivity measurements (single defects at helium temperature). Second, the measurements[35,36] on radiation damage in the electron microscope were both made on very thin foils (about 10^3 Å) and with high angular resolution. In contrast to this, our foils had thickness of more than 10^5 Å, and the angular width of the incident beam was very broad compared with the critical angles for channeling of electrons. Furthermore, we find both broad maxima and broad minima of the damage rate in the main crystallographic directions. A maximum in one direction is changed to a minimum and vice versa by varying the electron energy. In contrast to this the influence of channeling effects should only give very sharp maxima in damage rate for all main crystallographic directions independent of electron energy. Therefore, we can conclusively say that the influence of electron channeling on radiation damage, if existing at all, is negligible in our measurements because of foil thickness and beam spread.

V. DISCUSSION

In order to gain some qualitative insight into the connection between the threshold-energy profile and the measured orientation and energy dependence of the damage rate, the contributions of the different low-threshold-energy regions around the different main crystallographic axis have been calculated separately for the simplified profile outlined in Fig. 5. The results are plotted in Fig. 9.

At electron energies between 2 and 3 MeV, the displacement along directions around the ⟨111⟩ axis contributes most to the defect production, especially if the angular distance to the direction of the incident beam (and therefore also the cross section for energy transfer) is large. Other factors which influence the defect production are the size of the low-threshold-energy regions and the number of active regions which contribute to the defect production during irradiation in different crystallographic directions. For example, irradiation along the ⟨100⟩ axis results almost solely in displacements around the ⟨111⟩ directions (four active regions at an angular distance of 55° from the incident beam), whereas irradiation along the ⟨111⟩ axis results in displacements mainly around the ⟨100⟩ directions (three active regions at an angular distance of 55°) and around the oblique ⟨111⟩ directions (three active axes at an angular distance of 70° from the incident beam). Based on such simplified considerations of the contributions of the different active regions, the large differences of the observed dam-

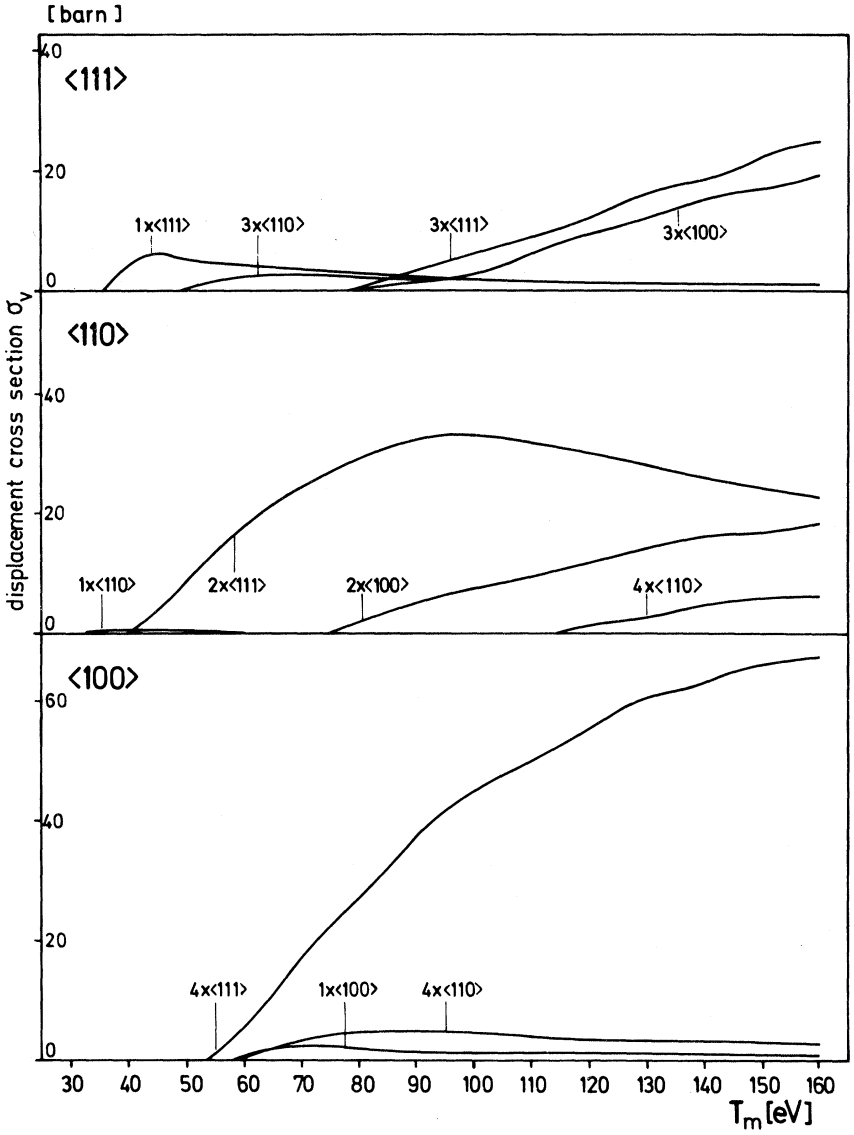

FIG. 9. Contributions of the low-threshold-energy regions around the main crystallographic axes of Fig. 5 to the damage rate for irradiation along the ⟨111⟩, ⟨110⟩, and ⟨100⟩ directions. The figures attached to the individual curves give the number and type of active regions for the displacement process.

age rates for irradiations along the different crystallographic directions can be understood qualitatively.

For a physical interpretation of the observed threshold-energy profile, a comparison with the results of computer simulations would be useful. Since such calculations do not exist for Ta, the results were compared with the calculation of Erginsoy *et al.*[32] for bcc iron (see Fig. 6). It is interesting to note that the topology of the calculated and observed profiles is very similar. However, the sequence in the average values of the threshold energies in the low-threshold-energy regions around the main crystallographic axes is different. For Ta, our experiments definitely show that displacement processes are easiest for recoils in and around the close-packed ⟨111⟩ direction.

This is just what one would expect if the interstitial of a stable Frenkel pair is produced via a replacement collision chain. These replacement collision chains are known to proceed best in the close-packed lattice directions.[37] Although the computer simulations have demonstrated that in all events in which stable Frenkel pairs are created the interstitial is indeed formed at the end of a replacement collision chain, nevertheless the computer threshold-energy profile does not show a minimum along the ⟨111⟩ but along the ⟨100⟩ direction in bcc iron. However, this result might be introduced artificially by the choice of the potential used for computer simulations. Among others, this choice has been based on the initial assumption that the threshold energy should show an absolute minimum near ⟨100⟩. This assumption was motivated by geometri-

cal considerations which predicted that the energy necessary to push an atom through the shell of its nearest-neighbor atoms is smallest for the ⟨100⟩ direction. Details of this so-called barrier model are given in Refs. 38 and 39. Obviously, the mere penetration of a recoil atom through the shell of its nearest-neighbor atoms is not a sufficient condition for the production of a stable Frenkel pair.

The computer simulation[32] as well as saturation-effect measurements[15] have clearly demonstrated that Frenkel pairs are stable only at larger separations of the interstitial and vacancy. In order to achieve this separation during the displacement process, replacement collisions are necessary. If this is true, it is not surprising that in tantalum the threshold energy for the defect production is indeed smallest in the close-packed lattice directions in which also the energy necessary for the initiation and propagation of replacement collision chains has its minimum value. Similar considerations have been rather successful also for the interpretation of the orientation dependence of the damage rates observed in semiconductors.[3-5]

ACKNOWLEDGMENTS

The authors are very grateful to R. Amadori for his advice and assistance in the numeric part of the calculations and to H. Hemmerich and the operating team of the Van de Graaff for experimental assistance. In addition, we would like to thank Chr. Lehmann and M. T. Robinson for many helpful discussions and for reading the manuscript.

[1]I. N. Haddad, P. C. Banbury, and J. A. Grimshaw, Phil. Mag. 12, 1203 (1965).

[2]I. N. Haddad and P. C. Banbury, Phil. Mag. 14, 829 (1966).

[3]P. C. Banbury and I. N. Haddad, Phil. Mag. 14, 841 (1966).

[4]P. C. Banbury, in *Radiation Effects in Semiconductors*, edited by F. L. Vook (Plenum, New York, 1968), p. 290.

[5]P. L. F. Hemment and P. R. C. Stein, in Ref. 4, p. 290.

[6]A. Sosin and K. Garr, Phys. Status Solidi 8, 481 (1965).

[7]K. Kamada, Y. Kazumata, and S. Suda, Phys. Status Solidi 7, 231 (1964).

[8]A. Sosin and W. Bauer, in *Studies in Radiation Effects in Solids*, edited by G. T. Dienes (Gordon and Breach, New York, 1969), Vol. 3, p. 153.

[9]J. N. Lomer and M. Pepper, Phil. Mag. 16, 1119 (1967).

[10]P. C. Banbury, J. N. Lomer, and E. W. J. Mitchell, in International Conference on Solid State Physics Research with Accelerators (BNL-50083), 1967, edited by A. Goland, p. 304 (unpublished).

[11]L. M. Howe, Phil. Mag. 22, 965 (1970).

[12]F. Maury, P. Vadja, A. Lucasson, P. Lucasson, G. Roux, and C. Minier, Phil. Mag. 22, 1265 (1970).

[13]E. H. Sondheimer, Advan. Phys. 1, 1 (1952).

[14]W. Bauer and A. Sosin, J. Appl. Phys. 35, 703 (1964).

[15]D. Meissner and W. Schilling, Z. Naturforsch. 26, 502 (1971).

[16]P. Jung, KFA Report No. Jül-729-FF, 1971 (unpublished).

[17]J. Hemmerich, KFA Report No. Jül-579-FN, 1969 (unpublished); and Z. Angew. Phys. 29, 1 (1970).

[18]J. Wurm, KFA Jülich, Report No. Jül-581-FN, 1969 (unpublished).

[19]J. Wurm, F. Dworschak, H. Schuster, and H. Wollenberger, Rad. Effects 5, 117 (1970).

[20]O. S. Oen, Oak Ridge National Laboratory Report No. ORNL-3813, 1965 (unpublished).

[21]J. W. Corbett, in *Solid State Physics Suppl.* 7, edited by F. Seitz and D. Turnbull (Academic, New York, 1966).

[22]G. Molière, Z. Naturforsch. 3a, 78 (1948).

[23]O. S. Oen, in Ref. 4, p. 264.

[24]C. N. Yang, Phys. Rev. 84, 599 (1951).

[25]H. Wenzl, in *Vacancies and Interstitials in Metals*, edited by A. Seeger, D. Schumacher, W. Schilling, and J. Diehl (North-Holland, Amsterdam, 1969), p. 363.

[26]K. Feese, D. Hoffmann, and H. Wollenberger, Cryst. Lattice Defects 1, 245 (1970).

[27]W. Köhler and W. Schilling, Nukleonik 7, 389 (1965).

[28]C. Erginsoy, G. H. Vineyard, and A. Shimizu, Phys. Rev. 139, A118 (1965).

[29]G. Youngblood, S. Myhra, and J. W. de Ford, Phys. Rev. 188, 1101 (1969).

[30]C. H. Sherman, L. F. Love, and E. A. Burke, Phys. Rev. 145, 568 (1966).

[31]R. van Jan and A. Seeger, Phys. Status Solidi 3, 465 (1969).

[32]C. Erginsoy, G. H. Vineyard, and A. Englert, Phys. Rev. 133, A595 (1964).

[33]P. G. Lucasson and R. M. Walker, Phys. Rev. 127, 1130 (1962).

[34]F. Frandsen and E. Uggerhøj, in International Conference on Atomic Collisions in Solids, Gausdal, Norway, 1971 (unpublished).

[35]M. J. Makin, in *Atomic Collision Phenomena in Solids*, edited by D. W. Palmer, M. W. Thomson, and P. D. Towsend (North-Holland, Amsterdam, 1970), p. 205.

[36]K. A. Shoaib and R. L. Segall, Phil. Mag. 22, 1269 (1970).

[37]G. Duesing and G. Leibfried, Phys. Status Solidi 9, 463 (1965).

[38]P. Lucasson and A. Lucasson, J. Phys. (Paris) 24, 503 (1963).

[39]H. H. Andersen and P. Sigmund, Risö-Report No. 103, 1965 (unpublished).